IMPULSIVE TIME-FREE TRANSFERS BETWEEN HALO ORBITS

L. A. Hiday* and K. C. Howell**
Purdue University
West Lafayette, Indiana

Abstract

A methodology is developed to design optimal time-free impulsive transfers between three-dimensional halo orbits in the vicinity of the interior L_1 libration point of the Sun-Earth/Moon barycenter system. The transfer trajectories are optimal in the sense that the total characteristic velocity required to implement the transfer exhibits a local minimum. Criteria are established whereby the implementation of a coast in the initial orbit, a coast in the final orbit, or dual coasts accomplishes a reduction in fuel expenditure. The optimality of a reference two-impulse transfer can be determined by examining the slope at the endpoints of a plot of the magnitude of the primer vector on the reference trajectory. If the initial and final slopes of the primer magnitude are zero, the transfer trajectory is optimal; otherwise, the execution of coasts is warranted. The optimal time of flight on the time-free transfer, and consequently, the departure and arrival locations on the halo orbits are determined by the unconstrained minimization of a function of two variables using a multivariable search technique. Results indicate that the cost can be substantially diminished by the allowance for coasts in the initial and final libration-point orbits.

I. Introduction

Trajectory design studies for scientific missions scheduled for launch in the 1990's have included investigations of the use of three-dimensional libration-point orbits in the vicinity of the interior L_1 libration point of the Sun-Earth/Moon barycenter system. With interest in such trajectories increasing, efficient transfers between libration-point orbits may offer more options and greater flexibility in trajectory design. Hence, this research effort is directed toward the formulation of a strategy to design optimal transfers between halo orbits near the L_1 libration point.

Associated with the general problem of minimum-fuel trajectories in an inverse square gravitational field is a well-developed theory stemming, in great part, from Lawden's pioneering work.[1] Formulating the problem of transferring a spacecraft between two points in the given gravitational field as a problem of Mayer in the calculus of variations, Lawden[2] states the necessary conditions that must be satisfied by the *primer vector* and its derivative on an impulsive trajectory that is considered optimal. The term primer vector is introduced by Lawden to denote the vector comprised of the adjoint variables associated with the velocity. If the primer magnitude exceeds unity at any instant on a reference trajectory, then this path is non-optimal and its cost can be reduced. Lion and Handelsman[3] and Jezewski and Rozendaal[4] extend the utility of primer vector theory by considering non-optimal impulsive trajectories whereby determining whether the addition of an interior impulse on a time-fixed transfer will improve the performance of a reference solution. Additionally, the location, magnitude, and direction of the additional impulse that render the greatest economy of fuel are specified.

Lion and Handelsman also establish criteria in accordance with which a coast in the initial orbit or a coast in the final orbit accomplishes a decrease in the cost function. The inclusion of either an initial or final coast on a reference solution produces a time-free transfer trajectory. (Note that the solution might also be discussed as a time-fixed transfer between specified endpoints that includes the option of initial and final coasts.) Several researchers, seeking minimum-fuel time-free trajectories in the two-body problem, employ various optimization techniques, including primer vector theory, in order to accomplish specific mission objectives such as transfers between near-circular orbits,[5,6] elliptical orbits,[7–9] and hyperbolic orbits,[10,11] as well as, direct ascent rendezvous of unconstrained duration,[12] and interplanetary transfers.[13,14] Transfers between two orbits in the three-body problem have been granted a modicum of consideration. Only very recently has primer vector theory been extended to the restricted three-body problem and applied to time-fixed transfers between two halo orbits in the vicinity of the L_1 libration point.[15]

Originally motivated by Pernicka's[16] examination of fuel-dumping transfers in conjunction with a potential near-term mission, this study investigates the determination, in the elliptic restricted three-body problem, of optimal time-free transfers between halo orbits near the L_1 libration point. The work contained herein augments the research presented in Ref. 15 by relaxing time-of-flight constraints through the introduction of coasts and by formulating the extension of primer vector theory to allow for the optimization of two-impulse time-free transfers. Here, optimum is defined to be minimum characteristic velocity or, equivalently, minimum of the sum of the magnitudes of

* Graduate Student, School of Aeronautics and Astronautics, Member AIAA.

** Associate Professor, School of Aeronautics and Astronautics, Senior Member AIAA.

the impulsive maneuvers. The solution for the optimal times of departure from the initial halo orbit and arrival in the final orbit are obtained using a multivariable search procedure. Since such methods essentially employ a gradient technique, the solution for the transfer converges only to a minimum within the same valley as the reference solution. Hence, the approach outlined here results in a locally optimal transfer trajectory, and other solutions may exist.

Since the time necessary to accomplish the transfer may be a critical factor in a mission, a comparison of the times of flight from a given initial orbit to a variety of final halo orbits is afforded. Additionally, the shifts of the departure and arrival locations on the halo orbits, as the amplitude of the final halo orbit varies, are examined. Once the best two-impulse time-free transfer is obtained, the optimality of this solution is examined, and the necessity of an additional impulse to reduce the total cost is ascertained. If an additional impulse is required, the optimization of the reference path proceeds with the time-fixed strategy developed in Ref. 15.

II. Force Model and Libration Point Trajectories

The model representing the actual forces acting on the spacecraft is chosen to be the elliptic restricted three-body model for the Sun-Earth/Moon barycenter system (i.e., Earth and Moon are considered a single body of mass equal to the sum of their individual masses placed at their barycenter). The initial and final libration-point orbits, between which a transfer is desired, are selected to be halo orbits, and upon specification of an injection date, the halo orbits are approximated using Richardson's[17] third order analytic approximation. The approximation for each halo provides the requisite initial estimate for the two-level iteration scheme in the numerical integration technique developed by Howell and Pernicka[18] which incorporates the eccentricity of the primary orbit. The resulting integrated halo trajectories are not exactly periodic; thus, they are not true halos as originally defined in the circular restricted problem. However, they render very close approximations, and the term 'halo orbit' usually encompasses such variations.

Next, the departure and arrival states on the integrated halo orbits are arbitrarily selected. The transfer path connecting these states is actually a portion of a Lissajous trajectory which can also be approximated utilizing the third order analytic approximation of Richardson and Cary.[19] Then this transfer trajectory is specified numerically by means of the previously identified integration scheme. The integrated Lissajous transfer is then patched between the two halo orbits so that the resulting complete trajectory (initial halo, transfer path, final halo) is continuous in position but contains two velocity discontinuities at the patch points. These differences in velocity on the halo orbits and the transfer path represent the $\Delta\bar{v}$'s necessary to implement the transfer. Since a transfer accomplished with the greatest economy of fuel is always desirable, a strategy to design optimal transfers is sought.

III. Formulation of the Optimization Problem

Let $\bar{x} = [x, y, z]^T$ and $\bar{v} = [v_x, v_y, v_z]^T$ represent a spacecraft's position and velocity, respectively, expressed in coordinates relative to the libration point and in the usual rotating frame associated with the restricted three-body problem. Then the equations of motion of the spacecraft between impulsive maneuvers (i.e., on a coastal arc) can be written in first-order form as

$$\dot{\bar{x}} = \bar{v}\,, \quad \dot{\bar{v}} = \bar{g}\,, \tag{1}$$

where

$$\bar{g} = \begin{bmatrix} 2nv_y + \dot{n}y + U_x \\ -2nv_x - \dot{n}x + U_y \\ U_z \end{bmatrix},$$

n is the angular velocity associated with the primary motion, and U_x, U_y, U_z are the first partial derivatives of the pseudo-potential U with respect to the position coordinates. The pseudo-potential is defined

$$U \triangleq \frac{1}{2}n^2(x^2 + y^2) + \frac{1-\mu}{d} + \frac{\mu}{r}\,,$$

where d and r represent the distances from the spacecraft to the Sun and to the Earth/Moon barycenter, respectively; also, μ denotes the mass ratio of this primary system. The position vector must be continuous; however, for impulsive trajectories, the velocity will be discontinuous at discrete instances. The optimality criterion, chosen to be the sum of the magnitudes of the velocity increments, is

$$J = \sum_k |\Delta\bar{v}_k|\,.$$

The Mayer-type optimization problem can then be stated as follows: Given an initial orbit A and a final orbit B, determine the transfer trajectory that connects these orbits such that the cost function J is minimized.

In order to treat the state equations (1) as differential constraints, Lagrange multipliers, called adjoint variables, are introduced. Let $\bar{\lambda}_x$ and $\bar{\lambda}_v$ denote adjoint vectors to the spacecraft's position and velocity, respectively. Then, the Hamiltonian H on a coastal arc in the elliptic restricted three-body problem takes the form

$$H = \bar{\lambda}_x^T\bar{v} + \bar{\lambda}_v^T\bar{g}\,,$$

and the differential equations governing the adjoints are written

$$\dot{\bar{\lambda}}_x^T = -\bar{\lambda}_v^T G_x$$
$$\dot{\bar{\lambda}}_v^T = -\bar{\lambda}_x^T - \bar{\lambda}_v^T G_v\,,$$

where

$$G_x \triangleq \frac{\partial \bar{g}}{\partial \bar{x}} = \begin{bmatrix} U_{xx} & U_{xy} + \dot{n} & U_{xz} \\ U_{xy} - \dot{n} & U_{yy} & U_{yz} \\ U_{xz} & U_{yz} & U_{zz} \end{bmatrix},$$

$$G_v \triangleq \frac{\partial \bar{g}}{\partial \bar{v}} = \begin{bmatrix} 0 & 2n & 0 \\ -2n & 0 & 0 \\ 0 & 0 & 0 \end{bmatrix},$$

and U_{ij} (i, j = x, y, z) are the second partial derivatives of the pseudo-potential.

Since $\bar{\lambda}_v$ plays an important role in formulating the necessary conditions for optimal trajectories, Lawden[2] introduces the term *primer vector* to denote the adjoint vector to the velocity; hence, $\bar{\lambda}_v$ will, hereafter, be denoted by the vector $\bar{p}$. Hiday and Howell[15] show that the primer vector, over a coastal arc from $t_0 \le t \le t_f$ in the elliptic restricted three-body problem, satisfies

$$\ddot{\bar{p}} = G_x \bar{p} + G_v \dot{\bar{p}} \qquad (2)$$

with boundary conditions

$$\bar{p}(t_0) = \frac{\Delta \bar{v}_0}{|\Delta \bar{v}_0|}, \quad \bar{p}(t_f) = \frac{\Delta \bar{v}_f}{|\Delta \bar{v}_f|}, \qquad (3,4)$$

where $\Delta \bar{v}_0$ and $\Delta \bar{v}_f$ are the impulsive maneuvers executed at the terminal points of the trajectory. The primer vector and its derivative transform in the same manner as the perturbations in position and velocity, so the solution of (2), given in terms of the partitioned state transition matrix associated with (1), is written as

$$\begin{bmatrix} \bar{p}(t) \\ \dot{\bar{p}}(t) \end{bmatrix} = \begin{bmatrix} \phi_{11}(t,t_0) & \phi_{12}(t,t_0) \\ \phi_{21}(t,t_0) & \phi_{22}(t,t_0) \end{bmatrix} \begin{bmatrix} \bar{p}(t_0) \\ \dot{\bar{p}}(t_0) \end{bmatrix}, \qquad (5)$$

where, as Lion and Handelsman[3] show, equations (2-4) uniquely define $\dot{\bar{p}}(t_0)$ as

$$\dot{\bar{p}}(t_0) = \phi_{12}^{-1}(t_f,t_0) \left[\bar{p}(t_f) - \phi_{11}(t_f,t_0)\, \bar{p}(t_0) \right] \qquad (6)$$

provided $\phi_{12}(t_f,t_0)$ is nonsingular. Hence, given initial conditions (3) and (6), the primer vector on a coastal arc is computed from equation (5).

Additionally, a very useful variational equation relating the perturbations in the state variables and $\bar{p}$ can be formulated. If δ symbolizes a contemporaneous variation, then Hiday and Howell[15] show that the primer vector, its derivative, and the perturbations in the state variables (i.e., $\delta\bar{x}$ and $\delta\bar{v}$) are related by the *adjoint equation*,

$$\bar{p}^T \delta\bar{v} - \left(\dot{\bar{p}}^T + \bar{p}^T G_v \right) \delta\bar{x} = \text{constant}, \qquad (7)$$

that is valid between the impulses on a trajectory in the elliptic restricted three-body problem. Adjoint equation (7) is the basis of much of the subsequent analysis.

The necessary conditions for an optimal time-fixed impulsive transfer trajectory, first developed by Lawden in conjunction with the two-body problem, are reformulated by Hiday and Howell[15] for the elliptic restricted three-body problem (i.e., for a gravitational field that is position-, velocity-, and time-dependent), and can be expressed entirely in terms of the primer vector as:

1. The primer vector satisfies $\ddot{\bar{p}} = G_x \bar{p} + G_v \dot{\bar{p}}$, and it must be continuous with continuous first derivative.
2. The magnitude of the primer vector is less than or equal to one during the transfer with impulses occurring at those instants for which $p = 1$.
3. At an impulse time, the primer vector is a unit vector aligned in the optimal thrust direction.
4. At all interior impulses (not at the initial or final times), $\dot{p} = 0$, and the derivative of the primer vector and the primer itself must be orthogonal (i.e., $\dot{\bar{p}}^T \bar{p} = 0$).

If a transfer trajectory connecting two orbits is not optimal, then an improved trajectory is sought.

IV. Criterion for an Initial Coast

Let Γ represent a two-impulse (reference) trajectory with terminal points $\bar{x}_0$ at $t = t_0$ on orbit A and $\bar{x}_f$ at $t = t_f$ on orbit B. Γ may be a complete trajectory or two-impulse segment of a multi-impulse trajectory. To test the efficacy of an initial coast to reduce the cost, the reference two-impulse trajectory is compared with a neighboring two-impulse (perturbed) trajectory Γ' that is allowed to coast ($dt_0 > 0$) in the initial orbit A. On Γ, impulses are applied at t_0 and t_f; whereas, Γ' remains on orbit A until $t_0 + dt_0$, and then impulses are applied at $t_0 + dt_0$ and t_f [See Figure 1]. Both trajectories reach the terminal state $\bar{x}_f$ on orbit B at t_f. Let the symbol 'd' represent a noncontemporaneous variation in a quantity, and denote a quantity on the perturbed trajectory with a prime. So, a noncontemporaneous variation in position is given by

$$d\bar{x} = \bar{x}'(t + dt) - \bar{x}(t).$$

Recall that δ represents a contemporaneous variation so that the first-order relationship between $d\bar{x}$ and $\delta\bar{x}$ is

$$d\bar{x} = \delta\bar{x} + \dot{\bar{x}}\, dt,$$

where $\delta\bar{x} = \bar{x}'(t) - \bar{x}(t)$. Now, the conditions under which Γ' can be realized are developed.

From Figure 1, the costs on Γ and Γ' are

$$J_\Gamma = |\bar{v}_0 - \bar{v}_A| + |\bar{v}_B - \bar{v}_f| \qquad (8)$$

$$J_{\Gamma'} = |\bar{v}_0' - \bar{v}_A'| + |\bar{v}_B - \bar{v}_f'|. \qquad (9)$$

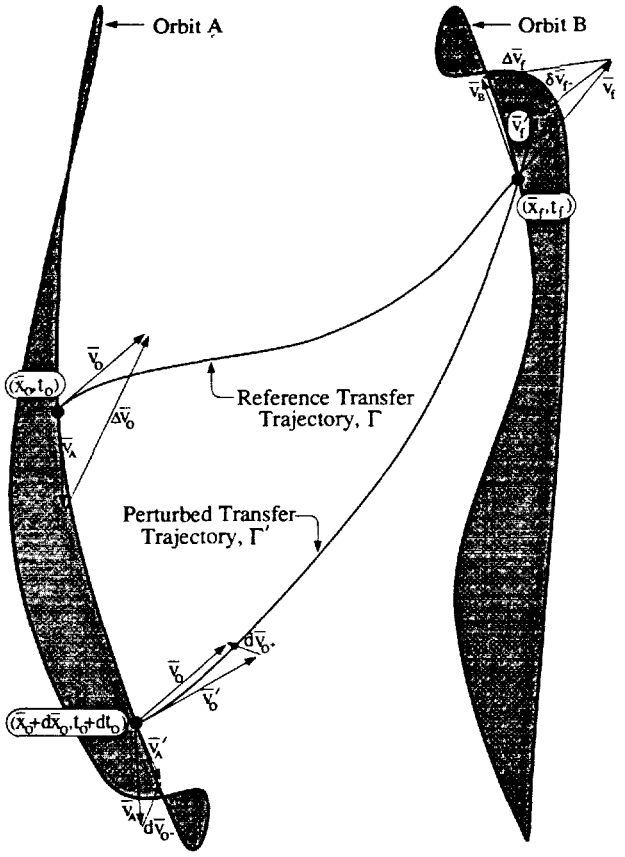

Fig. 1 Initial Coast Geometry

Employing the definitions of contemporaneous and noncontemporaneous variations, equation (9) can be rewritten as

$$J_{\Gamma'} = |(\bar{v}_0 + d\bar{v}_{0^+}) - (\bar{v}_A + d\bar{v}_{0^-})| + |\bar{v}_B - (\bar{v}_f + \delta\bar{v}_{f^-})| , \quad (10)$$

where subscripts $-$ and $+$ represent the one-sided evaluation of the corresponding quantity immediately before and immediately after, respectively, the specified terminal impulse. The criterion for the implementation of an initial coast is developed by considering the variation in the costs on Γ and Γ'; therefore, subtracting equation (8) from (10),

$$\delta J = |(\bar{v}_0 - \bar{v}_A) + (d\bar{v}_{0^+} - d\bar{v}_{0^-})| - |\bar{v}_0 - \bar{v}_A| + |(\bar{v}_B - \bar{v}_f) - \delta\bar{v}_{f^-}| - |\bar{v}_B - \bar{v}_f| .$$

Approximating the difference between the magnitudes of the initial and final impulses on Γ' and Γ to first order as outlined by Jezewski[20] and recalling that, at the endpoints of the reference trajectory, the primer vector is defined to have unit magnitude and to be aligned with the terminal impulsive maneuver simplifies the expression for the variation in cost to

$$\delta J = \bar{p}_0^T(d\bar{v}_{0^+} - d\bar{v}_{0^-}) - \bar{p}_f^T\delta\bar{v}_{f^-} . \quad (11)$$

Next, the utility of the adjoint equation, as it pertains to a perturbed trajectory that has been allowed to coast initially, is investigated. Recall that the adjoint equation is a contemporaneous variational expression that is valid everywhere on a coastal arc of a perturbed trajectory. Note that Γ' can be considered a single coastal arc that originates at $t = t_{0^+}$ and terminates at $t = t_{f^-}$. That the entirety of Γ' can be defined as a coastal arc should not be confused with the initial coast on orbit A. This initial coast on the perturbed trajectory is incorporated through the noncontemporaneous variation in time, dt_0. So, evaluating the variational relationship (7) over the duration of Γ',

$$@\ t = t_{0^+},\quad \bar{p}_0^T\delta\bar{v}_{0^+} - \left(\dot{\bar{p}}_0^T + \bar{p}_0^T G_{v_v}\right)\delta\bar{x}_{0^+} = C \quad (12)$$

$$@\ t = t_{f^-},\quad \bar{p}_f^T\delta\bar{v}_{f^-} - \left(\dot{\bar{p}}_f^T + \bar{p}_f^T G_{v_v}\right)\delta\bar{x}_{f^-} = C , \quad (13)$$

where C denotes the constant on the entirety of Γ'. Equating constants and noting that, since both the reference and perturbed trajectories reach the terminal state $\bar{x}_f$ on orbit B at t_f, $\delta\bar{x}_{f^-}$ must equal zero,

$$\bar{p}_0^T\delta\bar{v}_{0^+} - \left(\dot{\bar{p}}_0^T + \bar{p}_0^T G_{v_v}\right)\delta\bar{x}_{0^+} = \bar{p}_f^T\delta\bar{v}_{f^-} . \quad (14)$$

Additionally, the first-order relationships between the noncontemporaneous and contemporaneous variations in velocity immediately before and after the initial impulse at $t = t_0$ [See Figure 2] are written as

$$d\bar{v}_{0^-} = \delta\bar{v}_{0^-} + \dot{\bar{v}}_{0^-}dt_0 , \quad d\bar{v}_{0^+} = \delta\bar{v}_{0^+} + \dot{\bar{v}}'_{0^+}dt_0 , \quad (15,16)$$

where $\dot{\bar{v}}_{0^-}$ is the acceleration on orbit A prior to the the initial impulse on Γ', and $\dot{\bar{v}}'_{0^+}$ is the acceleration on Γ' after the initial impulse; however, to first order, the acceleration after the initial impulse can be calculated on the reference trajectory (i.e., $\dot{\bar{v}}'_{0^+} \simeq \dot{\bar{v}}_{0^+}$).[4] Also, since the velocity on both the reference and perturbed trajectories prior to $t = t_0$ is equivalent to the velocity associated with orbit A, $\delta\bar{v}_{0^-} = 0$. Hence, equations (15) and (16) can be rewritten to yield

$$d\bar{v}_{0^-} = \dot{\bar{v}}_{0^-}dt_0 , \quad d\bar{v}_{0^+} = \delta\bar{v}_{0^+} + \dot{\bar{v}}_{0^+}dt_0 . \quad (17,18)$$

Returning now to the first-order expression for the variation in cost, substituting equations (14), (17), and (18) into (11), and simplifying

$$\delta J = \bar{p}_0^T\left(\dot{\bar{v}}_{0^+} - \dot{\bar{v}}_{0^-}\right)dt_0 + \left(\dot{\bar{p}}_0^T + \bar{p}_0^T G_{v_v}\right)\delta\bar{x}_{0^+} . \quad (19)$$

Figure 3 illustrates that the contemporaneous variation in position at $t = t_{0^+}$ can be written in terms of the noncontemporaneous variation as

$$\delta\bar{x}_{0^+} = d\bar{x}_0 - \dot{\bar{x}}'_{0^+}dt_0 = d\bar{x}_0 - \bar{v}'_0 dt_0 ,$$

where the velocity on the perturbed trajectory $\bar{v}'_0$ is assumed equal to that on the reference trajectory, i.e., $\bar{v}'_0 = \bar{v}_0$. Recall that acceleration has previously been denoted by the symbol $\bar{g}$, so $\dot{\bar{v}}_{0^-}$ which is the acceleration on orbit A immediately prior to the initial impulse can be represented by the vector $\bar{g}_A$. Similarly, $\dot{\bar{v}}_{0^+}$, the acceleration on Γ immediately subsequent to the impulse at $t = t_0$, can be denoted by the vector $\bar{g}_0$.

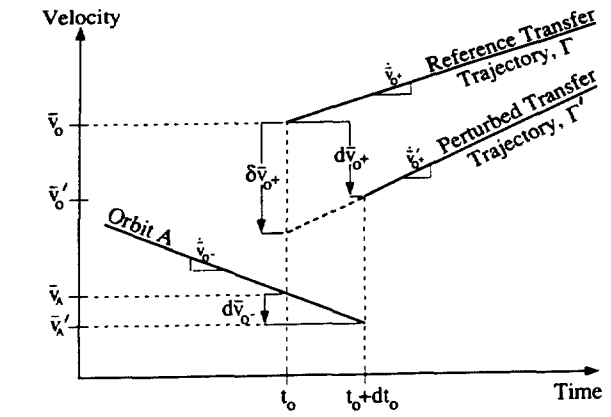

Fig. 2 Contemporaneous and Noncontemporaneous Velocity Variations

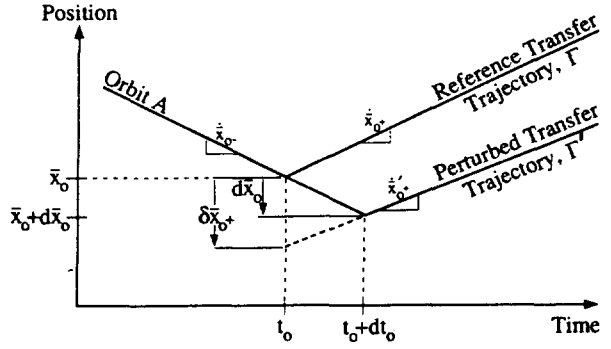

Fig. 3 Contemporaneous and Noncontemporaneous Position Variations

Making this notational change and substituting the above expression into (19),

$$\delta J = \bar{p}_0^T(\bar{g}_0 - \bar{g}_A - G_{v_0}\bar{v}_0)dt_0 + \dot{\bar{p}}_0^T(d\bar{x}_0 - \bar{v}_0 dt_0) + \bar{p}_0^T G_{v_0} d\bar{x}_0 \quad . \tag{20}$$

Notice that (20) contains the difference in acceleration across the initial impulse (i.e., $\bar{g}_0 - \bar{g}_A$). In contradistinction to the two-body problem, the acceleration in this formulation of the elliptic restricted three-body problem is a function of velocity; hence, acceleration is discontinuous across the impulse, and the quantity $\bar{g}_0 - \bar{g}_A$ is nonzero. So, the accelerations at the initial impulse must be examined in order to further simplify the expression for δJ.

Utilizing the definitions of $\bar{g}$ and G_v and owing to the continuity of the position vector, n, $\dot{n}$, and the partial derivatives of the pseudo-potential,

$$\bar{g}_0 - \bar{g}_A - G_{v_0}\bar{v}_0 = -G_{v_0}\bar{v}_A \quad . \tag{21}$$

Substituting (21) into equation (20),

$$\delta J = \dot{\bar{p}}_0^T(d\bar{x}_0 - \bar{v}_0 dt_0) + \bar{p}_0^T G_{v_0}(d\bar{x}_0 - \bar{v}_A dt_0) \quad . \tag{22}$$

Writing the noncontemporaneous variation in position at $t = t_0^-$ in terms of the contemporaneous variation,

$$d\bar{x}_0 = \delta\bar{x}_{0^-} + \dot{\bar{x}}_{0^-} dt_0 \; ;$$

however, since the reference and perturbed trajectories coincide initially on orbit A [See Figure 3], $\delta\bar{x}_{0^-}$ must equal zero and $\dot{\bar{x}}_{0^-}$ can be denoted $\bar{v}_A$. Hence,

$$d\bar{x}_0 = \bar{v}_A dt_0 \; ;$$

the last term in equation (22) is zero; and, the variation in the cost reduces to

$$\delta J = \dot{\bar{p}}_0^T d\bar{x}_0 - \left(\dot{\bar{p}}_0^T \bar{v}_0\right) dt_0 \quad . \tag{23}$$

Equation (23) represents the difference in cost between two neighboring trajectories whose initial positions differ by $d\bar{x}_0$ and initial times differ by dt_0. Because it is the analog of the transversality condition of the calculus of variations, equation (23) is called the *initial coast transversality condition*; however, (23) has wider applicability since neither Γ nor Γ' need be an optimum.

Now that the variation in cost between Γ and Γ' has been determined, the criterion for the inclusion of an initial coast, in an effort to reduce the cost, can be developed. Because the noncontemporaneous variation in the position of the initial impulse can be expressed solely in terms of the velocity on orbit A and the coastal period, the variation in cost can be rewritten as

$$\delta J = -\dot{\bar{p}}_0^T(\bar{v}_0 - \bar{v}_A)dt_0 \quad .$$

Since the coastal period is assumed to be positive (i.e., $dt_0 > 0$), then δJ can be made negative if, and only if,

$$\dot{\bar{p}}_0^T(\bar{v}_0 - \bar{v}_A) > 0 \quad .$$

However, from the primer vector boundary conditions which stipulate that $\bar{p}_0$ is parallel to $(\bar{v}_0 - \bar{v}_A)$ and $|\bar{p}_0| = 1$, the above inequality can be expressed as

$$\dot{p}_0 > 0 \quad , \tag{24}$$

where $\dot{p}_0$ symbolizes the slope of the primer vector magnitude at the instant of the initial impulse. So from (24), a reduction in cost can be achieved if the slope of a plot of the magnitude of the primer vector is positive at $t = t_0$. Hence, if the primer magnitude exceeds unity immediately after the initial impulse, an initial coast would lower the cost.

V. Criterion for a Final Coast

In a method analogous to the examination of the cost effectiveness of an initial coast, the variation in cost between the reference two-impulse trajectory and a neighboring two-impulse trajectory that is allowed to coast ($dt_f < 0$) in the final orbit B is examined in order to investigate the effect of a final coast. The impulses on Γ are still applied at t_0 and t_f; however, on Γ', the impulses are applied at t_0 and $t_f + dt_f$ such that the final coast in orbit B has duration $-dt_f$ [See Figure 4]. Both trajectories have initial states corresponding to $\bar{x}_0$ on orbit A at t_0. The variation in cost between Γ and Γ' is

$$\delta J = |(\bar{v}_0 - \bar{v}_A) + \delta\bar{v}_{0^+}| - |\bar{v}_0 - \bar{v}_A| + |(\bar{v}_B - \bar{v}_f) + (d\bar{v}_{f^+} - d\bar{v}_{f^-})| - |\bar{v}_B - \bar{v}_f| \quad ,$$

which, after considerable manipulation, reduces to

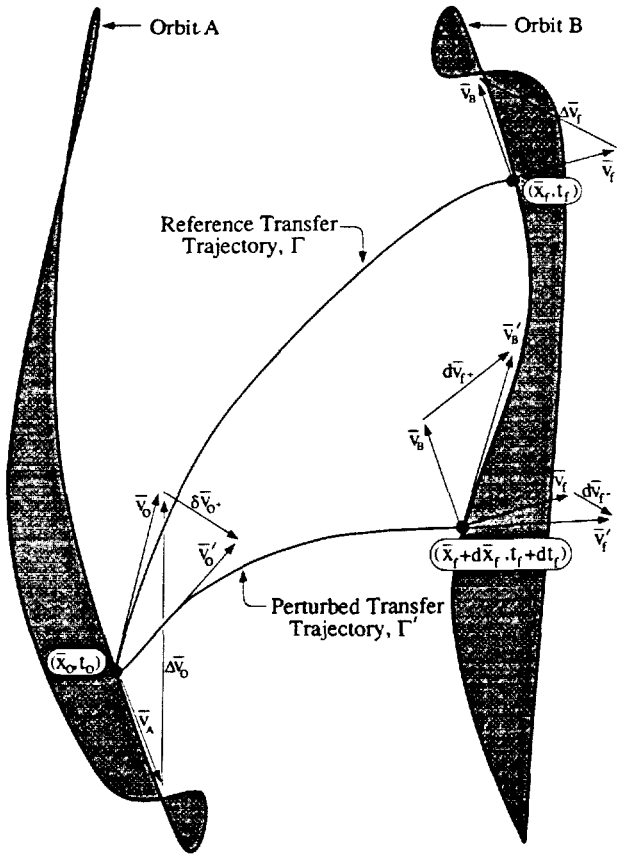

Fig. 4 Final Coast Geometry

$$\delta J = -\dot{\bar{p}}_f^T d\bar{x}_f + \left[\dot{\bar{p}}_f^T \bar{v}_f\right] dt_f \,. \qquad (25)$$

Equation (25) is the *final coast transversality condition* and represents, to first order, the difference in cost between two neighboring trajectories whose final positions differ by $d\bar{x}_f$ and final times differ by dt_f. Requiring the variation in cost to be negative such that a final coast on orbit B reduces the cost function J results in the criterion that

$$\dot{p}_f < 0 \,, \qquad (26)$$

where $\dot{p}_f$ symbolizes the slope of the primer vector magnitude at the instant of the final impulse. Thus, if the primer magnitude exceeds unity immediately prior to the final impulse, a final coast would lower the cost on the perturbed trajectory.

VI. Convergence to the Optimal Trajectory

If the reference two-impulse trajectory is non-optimal, then the coincident application of both an initial and final coast is explored as a means of reducing the total cost. This dual coast procedure results in a two-impulse transfer whose terminal points have been moved in time and, consequently, in position. Therefore, execution and optimization of a dual coast transfer yields the optimal time-free two-impulse transfer trajectory between variable endpoints on the given orbits A and B. Again, Γ represents the reference two-impulse trajectory with impulses at t_0 and t_f. In contrast, the impulses on the neighboring perturbed two-impulse trajectory Γ' are applied at $t_0 + dt_0$ and $t_f + dt_f$, where the restriction on the sign of the coastal periods is lifted so that dt_0 and dt_f can be either positive or negative. The terminology *initial coast* ($dt_0 > 0$) and *final coast* ($dt_f < 0$) is unaltered from the above analysis; however, if $dt_0 < 0$, the spacecraft executes an *early departure* from orbit A; additionally, if $dt_f > 0$, the spacecraft performs a *late arrival* on orbit B. For a given reference transfer trajectory, minimum fuel considerations render the optimal choices of sign for the coastal periods.

The difference in cost between the reference trajectory and the dual coast trajectory can be inferred from the independently-calculated cost variation for the initial coast and for the final coast trajectories of the preceding sections. So, the variation in cost between Γ and Γ' can be represented as

$$\delta J = \delta J \text{ (Initial Coast)} + \delta J \text{ (Final Coast)} \,, \qquad (27)$$

and, substituting the initial coast and final coast transversality conditions (23) and (25) into (27),

$$\delta J = \dot{\bar{p}}_0^T d\bar{x}_0 - \left[\dot{\bar{p}}_0^T \bar{v}_0\right] dt_0 - \dot{\bar{p}}_f^T d\bar{x}_f + \left[\dot{\bar{p}}_f^T \bar{v}_f\right] dt_f \,. \qquad (28)$$

Moreover, equation (28) is termed the *dual coast transversality condition*. Alternatively, expressing the noncontemporaneous variations in the positions of the terminal points in terms of orbital velocities and coastal periods, equation (28) simplifies to

$$\delta J = -\dot{\bar{p}}_0^T \Delta\bar{v}_0 dt_0 - \dot{\bar{p}}_f^T \Delta\bar{v}_f dt_f \,, \qquad (29)$$

where $\Delta\bar{v}_0 = \bar{v}_0 - \bar{v}_A$ and $\Delta\bar{v}_f = \bar{v}_B - \bar{v}_f$ represent the terminal velocity impulses. Next, recall that the primer vector at the endpoints of the trajectory is aligned with the impulsive velocity maneuver; hence, rearranging equations (3) and (4),

$$\Delta\bar{v}_0 = \bar{p}_0 |\Delta\bar{v}_0| \,, \quad \Delta\bar{v}_f = \bar{p}_f |\Delta\bar{v}_f| \,.$$

Replacing the velocity increments in (29) with the above expressions,

$$\delta J = -\dot{\bar{p}}_0^T \bar{p}_0 |\Delta\bar{v}_0| dt_0 - \dot{\bar{p}}_f^T \bar{p}_f |\Delta\bar{v}_f| dt_f \,.$$

Expressing the scalar product of the primer vector and its derivative as the product of the primer magnitude and the rate of change of this magnitude, then

$$\delta J = -\dot{p}_0 p_0 |\Delta\bar{v}_0| dt_0 - \dot{p}_f p_f |\Delta\bar{v}_f| dt_f \,, \qquad (30)$$

where p_0 and p_f denote the magnitude of the primer vector and $\dot{p}_0$ and $\dot{p}_f$ denote the slope of the magnitude of the primer vector at the initial and final impulse points, respectively. Since the primer vector is defined to have unit magnitude at the terminal points,

$$p_0 = p_f = 1 \,;$$

consequently, equation (30) simplifies to

$$\delta J = -\dot{p}_0 |\Delta\bar{v}_0| dt_0 - \dot{p}_f |\Delta\bar{v}_f| dt_f \,. \qquad (31)$$

So, equation (31) represents, to first order, the variation

in cost between the reference two-impulse trajectory and the perturbed, time-free two-impulse trajectory.

In order for a neighboring dual coast two-impulse trajectory having a lower cost than Γ to exist, δJ must be made negative; consequently,

$$-\dot{p}_0 |\Delta\bar{v}_0| dt_0 < \dot{p}_f |\Delta\bar{v}_f| dt_f . \qquad (32)$$

Whether criterion (32) is satisfied is dependent upon the sign of the coastal periods and the slope of the primer magnitude at the terminal points of the reference trajectory. For each combination of initial and final primer-magnitude slope, condition (32) renders the relationship between the coastal periods necessary for optimality. Also, the signs of the coastal periods are determined by compelling equation (31) to yield the largest negative variation in cost. The following four cases are representative of all possible combinations of non-zero initial and final slope of the primer magnitude:

- If $\dot{p}_0 > 0$ and $\dot{p}_f < 0$, then $dt_0 > 0$ and $dt_f < 0 \rightarrow$ Initial Coast/Final Coast.
- If $\dot{p}_0 > 0$ and $\dot{p}_f > 0$, then $dt_0 > 0$ and $dt_f > 0 \rightarrow$ Initial Coast/Late Arrival.
- If $\dot{p}_0 < 0$ and $\dot{p}_f < 0$, then $dt_0 < 0$ and $dt_f < 0 \rightarrow$ Early Departure/Final Coast.
- If $\dot{p}_0 < 0$ and $\dot{p}_f > 0$, then $dt_0 < 0$ and $dt_f > 0 \rightarrow$ Early Departure/Late Arrival.

If the initial and final slopes of the primer magnitude are zero, the trajectory is optimal.

Note that equation (31) can be written in the form

$$\delta J = \nabla J \cdot d\bar{z} ,$$

where $\bar{z}$ is a vector comprised of the times of the initial and final impulsive maneuvers. Thus, the problem of determining an optimal trajectory becomes one of minimizing $J(\bar{z})$ by a multivariable search method. Since the gradients are known analytically in terms of the initial and final impulses and the derivative of the primer vector at the terminal points of the reference trajectory, a minimizing technique that utilizes the gradient components is indicated. One such technique that has been employed is the Broydon-Fletcher-Goldfarb-Shanno (BFGS) variable metric method for unconstrained minimization which is available in the Automated Design Synthesis (ADS) package developed by Vanderplaats.[21]

Once the coastal periods that minimize the cost function are determined, the time of flight on the transfer trajectory is established and subsequently unmodified. The primer magnitude plot of the resultant transfer should display terminal points of zero slope. Additionally, if the primer magnitude, with the exception of the endpoints, lies entirely below unity, this two-impulse time-free transfer is optimal. However, should the primer magnitude exceed unity at any instant, then one or more impulsive maneuvers should be executed interior to the initial and final impulses such that the overall cost is diminished. Specification of the location, magnitude, and direction of the additional intermediate impulses is achieved utilizing the methodology developed for multi-impulse time-fixed transfers between libration-point orbits.[15]

VII. Results

As an application of the above method of constructing optimal time-free transfers, consider a trajectory that will move the spacecraft from an initial L_1 libration-point halo orbit characterized by a z-amplitude of 110,000 km to a final halo orbit, about the same libration point, with a z-amplitude of 160,000 km (Case A). The date of injection into the initial halo orbit at its point of maximum z-excursion is selected to be August 17. Departure from the initial halo and arrival at the final halo are initially chosen to occur near the minimum z-excursion point of each halo orbit. An analytic path that essentially connects the departure and arrival locations is determined to be a 1-rev Lissajous trajectory characterized by a y-amplitude of 373,972 km and a z-amplitude of 665,393 km. The complete trajectory, resulting from integration of the initial halo, the Lissajous transfer, and the final halo, is continuous in position but contains two velocity discontinuities representing a total $|\Delta\bar{v}|$ of 198.46 m/s. The time of flight (TOF) on the transfer segment of the complete trajectory is 175.98 days.

Next, the optimality of this reference two-impulse transfer is examined by computing the time history of the magnitude of the primer vector over the duration of the transfer segment of the reference trajectory [See Figure 5]. The slopes of the primer magnitude at the initial and final instants are clearly unequal to zero; hence, this two-impulse transfer is not optimal and can be improved by the inclusion of coasts on the initial and final halo orbits. Since the slope of the primer magnitude at the initial and final points on the reference solution are positive and negative, respectively, an initial coast ($dt_0 > 0$) and a final coast ($dt_f < 0$) are warranted. The coastal periods are optimized employing gradient information in the repeated utilization of the BFGS variable metric procedure in the ADS package. Figure 6 illustrates the y-z projection of the resultant two-impulse trajectory, which proceeds in a counter-clockwise direction. The origin of the plot corresponds to the oscillating L_1 libration point of the Sun-Earth/Moon system, and the axes shown in the figure are defined consistent with the rotating frame typically associated with the restricted three-body problem. The resulting coastal periods are $dt_0 = 3.15$ days and $dt_f = -40.11$ days and, in effect, move the arrival on the final halo orbit to a location near its minimum y-excursion while essentially leaving the departure from the initial halo unchanged from its minimum z-excursion point. This optimal two-impulse transfer is executed at a cost of 26.92 m/s and is accomplished in 132.72 days. Additionally, the corresponding primer magnitude time history, which is plotted relative to the time of flight on

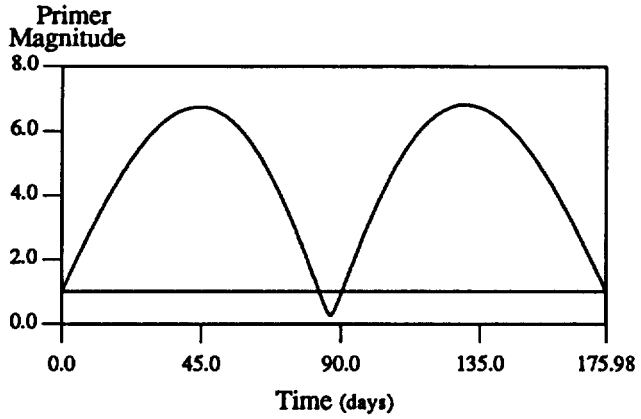

Fig. 5 Primer Magnitude History of 2-Impulse Nominal Transfer (Case A); $|\Delta\bar{v}|$ = 198.46 m/s

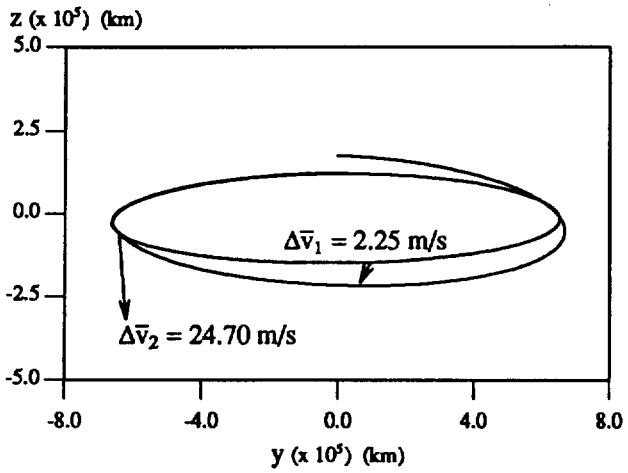

Fig. 6 y-z Projection of Optimal 2-Impulse Transfer (Case A); $|\Delta\bar{v}|$ = 26.96 m/s; Transfer TOF = 132.72 days

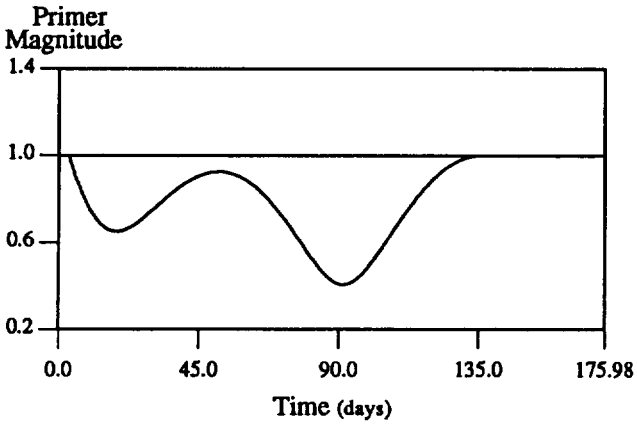

Fig. 7 Primer Magnitude History of Optimal 2-Impulse Transfer (Case A); $|\Delta\bar{v}|$ = 26.96 m/s

the reference transfer in order to illustrate the coastal periods [See Figure 7], complies with the necessary conditions for an optimal trajectory within the limitations of the multivariable search routine. Although the primer slope at the initial instant is apparently unequal to zero, the gradient of the cost function (comprised of the primer slope and the impulse magnitude) is quite small. Since the initial impulse is an order of magnitude smaller than the final impulse, the optimization process has difficulty rendering a solution that possesses primer slopes of comparable magnitude.

In order to determine what effect the size of the final halo orbit has on the optimal trajectory, transfers from the same initial halo orbit to two final halo orbits each of different size, characterized by z-amplitudes of 200,000 km and 240,000 km, are examined. For each of these transfers, the date of injection into the initial halo orbit is unchanged from August 17; moreover, the selection of the minimum z-excursions for the departure and arrival locations on the halo orbits is unaltered. Additionally, the sensitivity of the optimal solution to the original, non-optimal, two-impulse reference transfer is investigated by considering two different reference transfers to the same final halo orbit having a z-amplitude of 200,000 km. The first transfer (Case B) is determined according to the algorithm discussed previously; whereas, the second transfer (Case C) is determined using a crude type of continuation algorithm. Beginning with the Lissajous transfer path found for case A, the components of the velocity maneuvers are incrementally increased until a final halo orbit having a z-amplitude of 200,000 km is attained. The resulting non-optimal two-impulse transfers in cases B and C differ in velocity expenditure by approximately 14 m/s.

Both of these transfers along with the transfer to a halo orbit characterized by a z-amplitude of 240,000 km (Case D) exhibit non-optimal primer magnitude plots similar to that in Figure 5. (Note that the transfer path for case D is constructed in the same manner used to create the transfer for case C.) The cost on each transfer is then reduced by the execution of coasts in the initial and final halo orbits. The primer magnitude plots for cases B, C, and D are illustrated in Figures 8, 11, and 14, respectively. Notice that the times of flight on the resultant two-impulse time-free transfers are diminished substantially from the reference value of 177.20 days. In each case, the primer magnitude on the transfer portion of the trajectory lies, in part, above unity; hence, none of these transfers is optimal. However, as outlined in the time-fixed optimization strategy presented in Ref. 15, the total transfer cost can be further improved by the addition of an interior impulse. For case B, the resultant three-impulse transfer is optimal, and the corresponding y-z projection as well as the primer magnitude plot are illustrated in Figures 9 and 10.

In contrast, the three-impulse transfer trajectories for cases C and D violate the necessary condition that the primer magnitude not exceed unity [See Figures 13 and 16]; consequently, these transfers, whose y-z projections are shown in Figures 12 and 15, are non-optimal. Thus, another interior impulsive maneuver is implemented such that both transfers contain a total of four impulses, yet the execution of this additional interior impulse produces a minuscule percent variation in cost

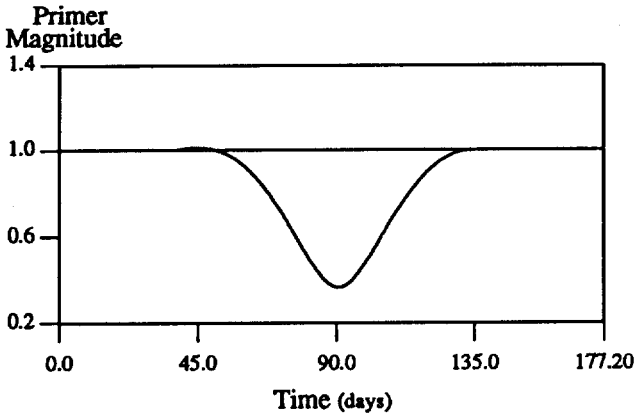

Fig. 8 Primer Magnitude History of Best 2-Impulse Transfer (Case B); $|\Delta\bar{v}|$ = 40.15 m/s

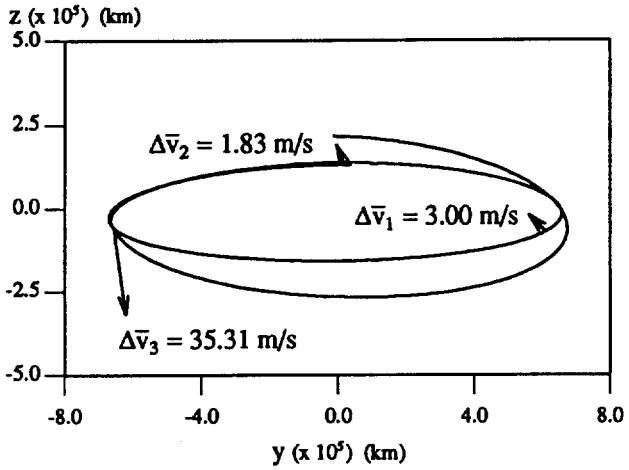

Fig. 9 y-z Projection of Optimal 3-Impulse Transfer (Case B); $|\Delta\bar{v}|$ = 40.14 m/s; Transfer TOF = 100.73 days

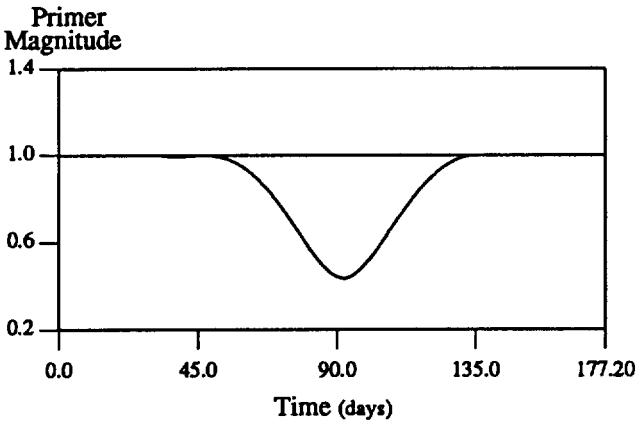

Fig. 10 Primer Magnitude History of Optimal 3-Impulse Transfer (Case B); $|\Delta\bar{v}|$ = 40.14 m/s

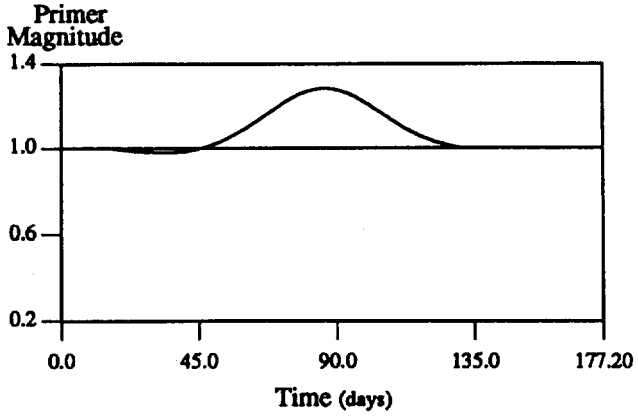

Fig. 11 Primer Magnitude History of Best 2-Impulse Transfer (Case C); $|\Delta\bar{v}|$ = 37.65 m/s

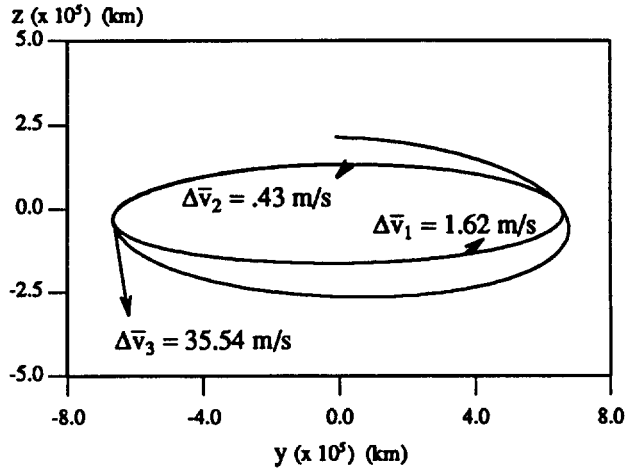

Fig. 12 y-z Projection of Best 3-Impulse Transfer (Case C); $|\Delta\bar{v}|$ = 37.59 m/s; Transfer TOF = 116.86 days

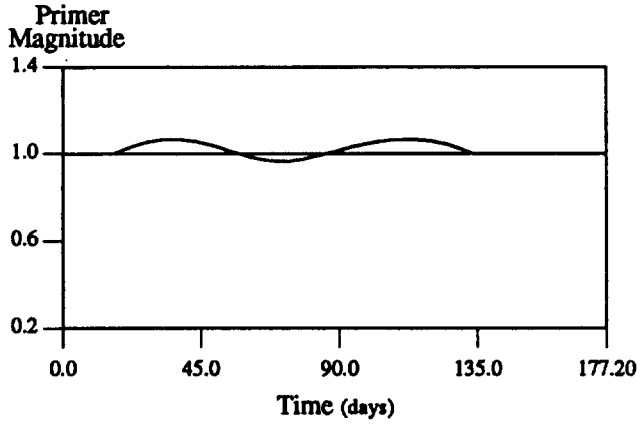

Fig. 13 Primer Magnitude History of Best 3-Impulse Transfer (Case C); $|\Delta\bar{v}|$ = 37.59 m/s

(–0.00215% for case C and –0.00011% for case D) and still yields a non-optimal solution. Consequently, for cases C and D, no significant gains are realized by the repeated addition of interior impulses in an effort to convergence to the *optimal* transfer trajectories; instead, the practical solutions illustrated in Figures 12 and 15, which accomplish the desired transfers with essentially the same cost in terms of $|\Delta\bar{v}|$ using only three impulses, are chosen to represent the *best* time-free impulsive transfers to their respective final halo orbits. Observe that the application of an interior impulse results in non-zero slopes at the endpoints of the primer

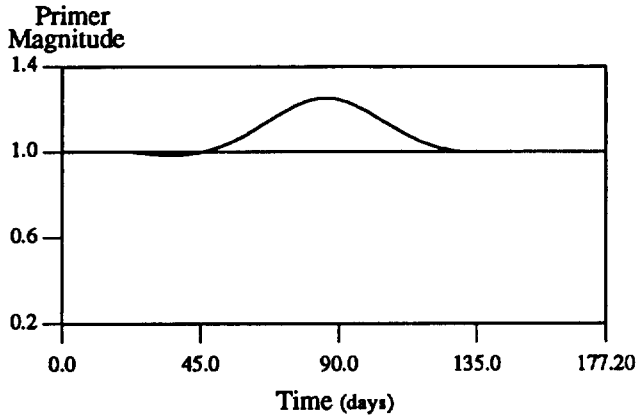

Fig. 14 Primer Magnitude History of Best 2-Impulse Transfer (Case D); $|\Delta\bar{v}|$ = 49.08 m/s

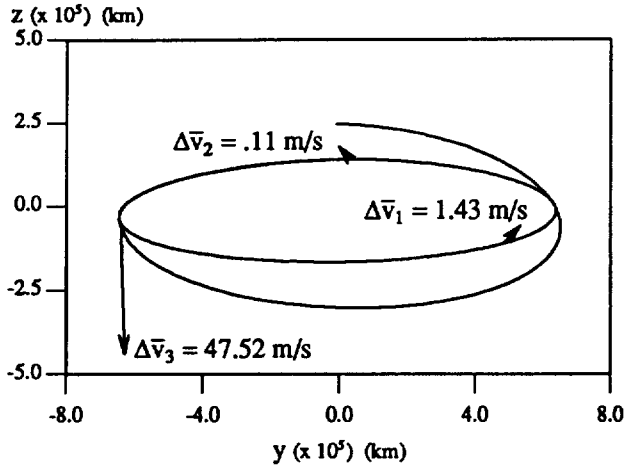

Fig. 15 y-z Projection of Best 3-Impulse Transfer (Case D); $|\Delta\bar{v}|$ = 49.06 m/s; Transfer TOF = 108.95 days

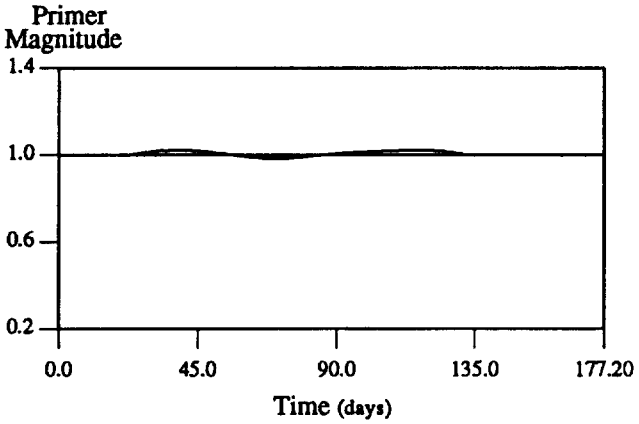

Fig. 16 Primer Magnitude History of Best 3-Impulse Transfer (Case D); $|\Delta\bar{v}|$ = 49.06 m/s

magnitude histories plotted in Figures 13 and 16. Restoration of the slopes to zero would require the simultaneous optimization of the coastal periods and the timing and location of the interior impulse, but such an approach destroys the integrity of the numerical solutions for the initial and final halo orbits. Thus, once the coastal periods are determined, they are subsequently unaltered. This omission of coastal period modification during the application and optimization of the interior impulse is responsible, in part, for the difficulty in obtaining optimal solutions.

Notice that for all four optimal or best transfers (cases A-D) the initial impulse as well as the intermediate impulse (if applicable) are small in magnitude and variable in orientation; whereas, the final impulse is quite large and oriented out-of-plane. For each of the transfers considered, the initial and intermediate impulses act to perturb the spacecraft's initial trajectory precisely so that the transfer intersects the final halo orbit near its minimum y-excursion point. At this location, a single impulse of significant magnitude is then sufficient to complete the transferal of the spacecraft to the desired final orbit. Hence, these time-free transfers perform the majority of the transition between the halo orbits in the third quadrant of the y-z plane; remarkably, the optimal multi-impulse time-fixed transfer trajectories constructed in Ref. 15 similarly exhibit this phenomenon of predominantly third-quadrant transferal.

Table 1 summarizes the fuel expenditures for the four cases that are investigated. The time-free transfers demonstrate a dramatic reduction in the total cost compared to the non-optimal two-impulse reference solutions. Excepting case B, the cost on the optimized transfer trajectory increases nearly linearly with z-amplitude of the final halo orbit; also, with each successive increase in z-amplitude, the time of flight on the transfer decreases thereby delaying departure from the initial halo orbit and advancing departure location toward the initial halo's maximum y-excursion. Case C, the reference transfer that requires less $|\Delta\bar{v}|$ to reach the final halo orbit with z-amplitude of 200,000 km, results in a three-impulse transfer, albeit non-optimal, having a significantly lower cost than its counterpart, case B. Hence, the relatively anomalous cost in case B, which is also demonstrated in the corresponding time-fixed transfer, is explained by the fact that the cost on the optimal time-free transfer is sensitive to the reference two-impulse solution from which the optimal transfer is derived.[15] Also, increasing the flexibility of the design strategy presented in Ref. 15 by relaxing time-of-flight constraints results in time-free transfers possessing lower cost than the comparable time-fixed transfers.

VIII. Summary

This study involves the successful development of a methodology for the design of optimal time-free impulsive transfer trajectories between variable endpoints on halo orbits in the vicinity of the interior L_1 libration point of the Sun-Earth/Moon barycenter system. The strategy outlined above is enabled by the extension of primer vector theory to non-optimal trajectories in the elliptic restricted three-body problem whereby the implementation of coasts on the initial and

Table 1 Costs On Time-Free Transfers To Various Final Halo Orbits

Case	Z-Amplitude of Initial Halo (km)	Z-Amplitude of Final Halo (km)	Nominal 2-Impulse Transfer $\|\Delta\bar{v}\|$ (m/s)	Nominal 2-Impulse Transfer TOF (days)	Optimized Time-Free Transfers 2-Impulse $\|\Delta\bar{v}\|$ (m/s)	Optimized Time-Free Transfers 3-Impulse $\|\Delta\bar{v}\|$ (m/s)	Optimized Time-Free Transfers TOF (days)
A	110,000	160,000	198.46	175.98	26.96	NA	132.72
B	110,000	200,000	400.49	177.20	40.15	40.14	100.73
C	110,000	200,000	386.59	177.20	37.65	37.59†	116.86
D	110,000	240,000	447.32	177.20	49.08	49.06†	108.95

† Resultant trajectory is non-optimal.

final orbits is considered as a means of reducing the cost in terms of maneuver $|\Delta\bar{v}|$'s. Results indicate that a substantial savings in total $|\Delta\bar{v}|$ can be achieved by the allowance for coastal periods on the halo orbits. Future efforts may involve the in-depth analysis of the variability of times of flight and of shifts in departure and arrival locations as the amplitudes of the libration-point orbits are altered.

IX. References

1. Lawden, D. F., "Rocket Trajectory Optimization: 1950-1963," *Journal of Guidance, Control, and Dynamics*, Vol. 14, No. 4, July-August 1991, pp. 705-711.
2. Lawden, D. F., *Optimal Trajectories for Space Navigation*, Butterworths, London, 1963.
3. Lion, P. M. and Handelsman, M., "Primer Vector on Fixed-Time Impulsive Trajectories," *AIAA Journal*, Vol. 6, No. 1, January 1968, pp. 127-132.
4. Jezewski, D. J. and Rozendaal, H. L., "An Efficient Method for Calculating Optimal Free-Space N-Impulse Trajectories," *AIAA Journal*, Vol. 6, No. 11, November 1968, pp. 2160-2165.
5. Marec, J. P., "Transferts Infinitesimaux Impulsionnels Economiques Entre Orbites Quasi-Circulaires Non Coplanaires," *Astronautica Acta*, Vol. 14, No. 1, November 1968, pp. 47-55.
6. Edelbaum, T. N., "Minimum Impulse Transfers in the Near Vicinity of a Circular Orbit," *The Journal of the Astronautical Sciences*, Vol. 14, No. 2, March-April 1967, pp. 66-73.
7. Marchal, C., "Transferts Optimaux Entre Orbites Elliptiques (Durée Indifférente)," XVI IAF Congress, Athens, 1965.
8. Gobetz, F. W., Washington, M., and Edelbaum, T. N., "Minimum-Impulse Time-Free Transfer Between Elliptic Orbits," NASA CR-636, November 1966.
9. Marec, J. P., "Optimal Transfers Between Close Elliptical Orbits," NASA TT F-554, September 1969.
10. Gobetz, F. W., "Optimum Transfers Between Hyperbolic Asymptotes," *AIAA Journal*, Vol. 1, No. 9, September 1963, pp. 2034-2041.
11. Marchal, C., "Transferts Optimaux Entre Orbites Hyperboliques (Rayon Planétaire Non Nul)," XVII IAF Congress, Madrid, 1966.
12. Carstens, J. P. and Edelbaum, T. N., "Optimum Maneuvers for Launching Satellites into Circular Orbits of Arbitrary Radius and Inclination," *ARS Journal*, Vol. 31, No. 7, July 1961, pp. 943-949.
13. Marchal, C., "Analytical Comparison of the Successive Planetary Windows in the Study of the Economical Earth-Planet Transfers," XIX IAF Congress, New York, 1968.
14. Gravier, J. P., Marchal, C., and Culp, R. D., "Optimal Impulsive Transfers Between Real Planetary Orbits," *Journal of Optimization Theory and Applications*, Vol. 15, No. 5, May 1975, pp. 587-604.
15. Hiday, L. A. and Howell, K. C., "Transfers Between Libration-Point Orbits in the Elliptic Restricted Problem," AAS/AIAA Space Flight Mechanics Conference, Colorado Springs, Colorado, February 24-26, 1992.
16. Pernicka, H. J., "The Numerical Determination of Nominal Libration Point Trajectories and Development of a Station-Keeping Strategy," Ph.D. Dissertation, School of Aeronautics and Astronautics, Purdue University, May 1990.
17. Richardson, D. L., "Analytic Construction of Periodic Orbits About the Collinear Points," *Celestial Mechanics*, Vol. 22, 1980, pp. 241-253.
18. Howell, K. C. and Pernicka, H. J., "Numerical Determination of Lissajous Trajectories in the Restricted Three-Body Problem," *Celestial Mechanics*, Vol. 41, 1988, pp. 107-124.
19. Richardson, D. L. and Cary, N. D., "A Uniformly Valid Solution for Motion About the Interior Libration Point of the Perturbed Elliptic-Restricted Problem," AIAA/AAS Astrodynamics Specialist Conference, AAS 75-021, Nassau, Bahamas, July 28-30, 1975.
20. Jezewski, D. J., "Primer Vector Theory and Application," NASA TR R-454, November 1975.
21. Vanderplaats, G. N., *ADS—A Fortran Program for Automated Design Synthesis*, Version 1.10, May 1985.